RSC Applied Polymers

ROYAL SOCIETY OF CHEMISTRY

PAPER

View Article Online
View Journal | View Issue

Cite this: *RSC Appl. Polym.*, 2023, **1**, 325

Pristine coconut husk biowaste and 2-ethylhexyl acrylate/methyl acrylate-based novel oleophilic gels for oil spill cleanup

Kavita Devi,[a] Ghanshyam S. Chauhan, [a] Sunita Ranote, [b] Sandeep Chauhan*[a] and Kiran Kumar *[a]

Oil pollution due to accidental oil spills and unethical industrial discharge into the aquatic system has been a major problem for decades. Industrialization and urbanization have made us dependent on petroleum products for survival. Hence, with the augmented transportation of these oil products, incidents of oil spill accidents have now become common. Water pollution due to these spills drastically affects aquatic and terrestrial life. Thus, it necessitates the use of economical and eco-friendly biosorbents for oil spill remediation. Herein, we report the synthesis of efficient oleophilic gels based on pristine coconut husk (C^h) and acrylate monomers [2-ethylhexyl acrylate and methyl acrylate] using the free radical polymerization technique with potassium persulfate (KPS)-*N*,*N*′-methylenebisacrylamide (MBA) as an initiator–crosslinker system. The synthesized oleophilic gels were characterized further using different techniques. The adsorption of various petroleum products such as toluene, petroleum ether, petrol, and diesel from their respective oil–water emulsions has been studied. The polymers poly(EHA)-*cl*-C^h and poly(MA)-*cl*-C^h synthesized with 2% [MBA] showed maximum adsorption capacities of 15.2 g g^{-1} and 13.0 g g^{-1}, respectively, within 60 min at 35 °C, which is far better than pristine coconut husk which showed an adsorption capacity of only 2.1 g g^{-1} under the same conditions. The kinetics data best fitted in the pseudo-second-order kinetics model. The oleophilic gels were found to be reusable with appreciable adsorption of up to six cycles of regeneration. The cumulative adsorption capacities of poly(EHA)-*cl*-C^h and poly(MA)-*cl*-C^h were found to be 50.0 g g^{-1} and 35.2 g g^{-1}, respectively. The effect of salinity on the adsorption capacity was also investigated using varied brine water emulsions. The oleophilic gels showed comparable adsorption capacities of 15.0 g g^{-1} and 12.2 g g^{-1} for poly(EHA)-*cl*-C^h and poly(MA)-*cl*-C^h, respectively, at a lower brine water concentration (1%). At a higher concentration of brine solution (5%), appreciable adsorption capacities of 12.8 g g^{-1} and 10.4 g g^{-1} were reported. A comparison between the two monomers clearly depicted the increase in the oleophilic capacity with the increase in the hydrocarbon chain. The synthesized oleophilic gels are, therefore, suitable candidates for dealing with oil spill cleanup.

Received 21st July 2023,
Accepted 28th September 2023

DOI: 10.1039/d3lp00118k

rsc.li/rscapplpolym

1. Introduction

Petroleum is one of the most useful non-renewable resources that fulfill our energy needs. The boom in industrialization, urbanization, and population has led to increasing dependency on petroleum-based hydrocarbons. The transportation of these petroleum products, mostly through sea routes, has also witnessed a huge upsurge. With such enormous transportation, the problem of oil spilling is one of the major concerns in front of us. Oil spilling into the aquatic environment may occur either operationally or accidentally *e.g.*, due to their shipping through oceans, offshore oil well explosions,[1] and waste disposal of oil refineries. Natural oil seepages are estimated to be 18 million gallons around the globe per annum.[2] Oil spills not only cause water and soil pollution worldwide but also have jeopardous effects on the economy, tourism, and human health. Oil inhibits the penetration of sunlight into the water and affects the aquatic flora by restricting photosynthesis. Oil droplets trap minute organisms by acting as a flypaper and ultimately kill them, thereby disturbing the aquatic food chain. Oil droplets also affect fish by sticking onto their gill surfaces causing breathing problems. Consumption of such

[a]*Department of Chemistry, Himachal Pradesh University, Summer-Hill, Shimla, Himachal Pradesh, India. E-mail: kgrewalcg@gmail.com, drkiran@hpuniv.ac.in, sandeepchauhanin2020@gmail.com*
[b]*Centre of Polymer and Carbon Materials, Polish Academy of Sciences, 34. M. Curie-Sklodowska St., 41-819 Zabrze, Poland*

contaminated water and aquatic organisms leads to fatal toxic effects on humans as these oil contaminants have low boiling points and are carcinogenic. Various examples have been reported where lives were catastrophically affected by oil spills.[3–5] It is estimated that around 100 000 and 500 000 seabirds are killed due to oil pollution every winter season in the North and Baltic Seas.[6] Significant oil spills have been reported along the Nile River in recent years.[7] Thermal and photochemical degradation of hydrocarbons results in the release of nutrients into the water that increase algal growth, which prevents the development of mussels with plankton larvae around them.[2] Oil dispersion in water occurs at a very high speed and further undergoes various processes like spreading, emulsification, evaporation, photooxidation, sinking, dissolution, and tarball formation.[8] Thus, there is an urgent need for the remediation of such oil spills from water resources. Many physicochemical, thermal, and biological methods have been employed for oil spill cleanup.[9] Physical methods prevent oil spread using physical barriers such as booms, skimmers, and adsorbents.[6] Chemical methods use solidifiers and dispersants to change the chemical nature of oils and make their removal easy. All these physicochemical methods prove to be very costly and a financial burden on government resources. Microbes are employed for the degradation of oil droplets in the case of biological methods and the thermal process involves the *in situ* burning of these liquids.[6] There are limitations associated with every method. The most common and cost-effective method is using biomass-based polymeric absorbents for the sorption of oil from the oil–water system due to their low cost, high abundance, reusability, biodegradability, and high surface area.[10] A variety of lignocellulosic biowastes have been used for oil spill removal, *e.g.*, Ali *et al.* reported the synthesis of oleophilic gels from *n*-butyl acrylate for oil spill cleanup.[11] Gum tragacanth, a natural polysaccharide, was grafted with acrylic acid and methylmethacrylate by Saruchi *et al.* for oil spill remediation.[12] He *et al.* proposed the utilization of aerogels derived from carboxymethylated chitosan which showed remarkable oil adsorption capacities along with excellent regeneration ability.[13] Jayaramulu and his co-workers synthesized oleophilic metal–organic nanofibrous gel composites for oil adsorption.[14] Tayeb *et al.* utilized natural biowaste rice straw for the sorption of crude oil from seawater which showed a maximum sorption capacity of 6.6 g g^{-1}.[15] Asadpour *et al.* studied the adsorption behavior of modified corn silk for crude oil uptake.[16] Similarly, palm fibers,[17] banana peels,[18] sugarcane bagasse,[19] and coir[20] have been used for such oil spill remediation applications. Most of the natural biomasses are found to be less hydrophobic and exhibit less selectivity for hydrocarbons. But these can be tailored physically, chemically, or thermally to enhance their oil uptake ability. The chemical modifications were found to be most useful to synthesize water-repellant sorbents by introducing hydrophobic moieties into their structures.[7] Hydrophilic sawdust upon reaction with octadecyl trichlorosilane was proved to be oleophilic due to the silylation of –OH groups with highly hydrophobic trioctyl groups.[21] Biochar obtained from the leaves of *Populus nigra* was found to be an efficient absorbent of oils.[22] Michael-igolima and co-workers modified orange peel waste by physical, chemical, and thermal methods. Each of the modified products showed a higher sorption capacity than non-treated biowaste and the best results for oil uptake were shown by the one modified chemically.[23] Similarly, various sorbent materials were synthesized and used for oil spill cleanup.[24–29] Crosslinking and various polymer analogous reactions have been used to tailor these bio-wastes for such oil spill applications.[30,31] Using biowaste can also serve to tackle another major problem: its disposal and environmental pollution. Globally, a large amount of biowaste is produced. Untreated biowaste not only pollutes the air, water, and soil but also poses a serious threat to human health and the biosphere as a whole. These biowastes can be made useful with some modifications as has been reported earlier.[32–34] In the present research article, we have used pristine coconut husk for the study as it is highly abundant and cost-effective. In 2019, after Indonesia and the Philippines, India was the third largest coconut producer in the world, with around 14.68 million metric tonnes of total production.[35] Such huge production of coconut all over the world leads to the massive production of waste coconut husk, shell, and fibers. Coconut husk (*Cocos nucifera*) is a lignocellulosic biomass that is made up of lignin (43.81%), cellulose (24.26%), and hemicellulose (20.54%).[36] There are various reports where coconut husk (coir) has been modified for various wastewater treatment applications for the removal of toxic dyes, metal ions, and petroleum-based hydrocarbons/oils.[37,38] Herein, pristine coconut husk has been modified to introduce hydrophobicity by crosslinking with different acrylate monomers using the free radical polymerization technique. Comparative studies were performed on coconut husk and acrylate monomer-based polymeric networks with varied crosslinker concentrations to test their ability to remove different petroleum-based candidate products such as toluene, petroleum ether, petrol, and diesel. Petrol and diesel are the most common petroleum products used as fuel in the transport sector and the oil-spill incidents during their transportation are quite large. Toluene and petroleum ether are harmful volatile organic compounds (VOCs) resulting from the chemical synthesis or extraction steps in various industrial processes. So, taking into account their harmful effects and vast use in different fields, these products were chosen as candidate petroleum products. The literature survey also revealed the necessity for the removal of these harmful VOCs.[39–44] The selection of acrylate monomers is based on their low cost, biocompatibility, easy functionalization,[45] and very high affinity for oils and organic, aromatic, and chlorinated solvents.[46]

Based on the above observations, the main objective of the present study is the functionalization of pristine coconut husk with ethylhexyl acrylate (EHA) and methyl acrylate (MA) using the free radical polymerization technique with potassium persulfate (KPS)-*N*,*N*′-methylenebisacrylamide (MBA) as an initiator–crosslinker system for use in oil cleanup application. The synthesized polymers were designed and modified with

the aim of making them highly efficient for oil spill cleanup applications. The incorporation of hydrophobic hydrocarbon moieties into the backbone was assumed to increase the adsorptive interactions between the candidate petroleum products *viz.* toluene, petroleum ether, petrol, and diesel chosen for the study and the synthesized polymer matrix. The network formation was confirmed by characterization studies using Fourier transform infrared spectroscopy (FTIR), field emission scanning electron microscopy (FE-SEM), energy-dispersive X-ray spectroscopy (EDS), and X-ray diffraction (XRD) analysis. The uptake behavior of the synthesized polymers in various oil–water emulsions has been established using various kinetic models. This research work is novel as no such work having modified pristine coconut husk with acrylate monomers for such application has been reported to the best of the author's knowledge.

2. Experimental

2.1. Materials

Coconut husk (C^h) (obtained from the local market, Shimla, India), 2-ethylhexylacrylate (EHA) and methyl acrylate (MA) (TCI Japan), potassium persulfate (KPS) and *N*,*N*′-methylenebisacrylamide (MBA) (S.D. Fine Chem Ltd India), toluene and petroleum ether (TCI Japan), and petrol and diesel (locally available) were all of analytical grade and used as received. The solvents were double-distilled before use.

2.2. Synthesis of poly(EHA)-*cl*-C^h and poly(MA)-*cl*-C^h

C^h was washed thoroughly with distilled water and dried for 12 h at 40 °C. Finely powdered C^h (1 g) was then immersed in distilled water for 12 h and then mixed with varied amounts of KPS, MBA, and EHA/MA. The above reaction mixtures were continuously stirred to form homogeneous mixtures and kept at an optimized temperature until solid polymeric masses were formed. The resultant crosslinked masses, poly(EHA)-*cl*-C^h and poly(MA)-*cl*-C^h, were then washed thoroughly with water and ethanol to remove any homopolymers formed. The synthesized materials were further equilibrated with distilled water for 24 h to remove any water-soluble impurities. They were then filtered and dried in a hot air oven at 35 °C. The dried samples were finely powdered and used for further oil-sorption experiments. Different reaction conditions such as temperature, time, monomer, and crosslinker concentrations were optimized to achieve maximum % grafting (P_g). P_g was calculated using an earlier reported expression.[47]

2.3. Characterization studies

The incorporation of EHA and MA into C^h to form poly(EHA)-*cl*-C^h and poly(MA)-*cl*-C^h was confirmed by various characterization techniques such as FTIR spectra (PerkinElmer FTIR spectrometer) in the range of 4000–400 cm^{-1} using KBr pellets, XRD patterns on a Philips PAN Analytical XPERT-PRO and FESEM images recorded on an SEM digital scanning electron microscope JSM 6100 (JEOL) and elemental mapping.

2.4. Adsorption studies

C^h and different polymers, synthesized separately at varied crosslinker concentrations (2%, 5%, 7%, and 10%) for both the monomers, EHA and MA, were studied for the adsorption of different oil products and solvents such as toluene, petroleum ether, petrol, and diesel in their respective emulsions with water using the gravimetric method. Pre-weighed C^h (50 mg) and dried polymer samples (50 mg each) were separately added to beakers containing oil–water emulsions. Each beaker was subjected to magnetic stirring to maintain proper emulsion during adsorption. The final weight of each sample was recorded after a specified time of immersion in the solvent–water emulsion.

Batch experiments were performed to obtain the optimized conditions of time (15–150 min) and temperatures (25–45 °C) for adsorption of the synthesized polymers in different oil–water emulsions. Adsorption capacity (q) and %solvent uptake (P_u) were calculated using the following expressions:[48–50]

$$\text{Absortion capacity } (q) = \frac{(w_2 - w_1)}{w_1}$$

$$\text{Percent solvent uptake } (P_u) = \frac{(w_2 - w_1)}{w_1} \times 100$$

where 'q' is the sorption capacity of samples in g g^{-1} and 'w_1' and 'w_2' are the weights of the samples in grams before and after adsorption, respectively. 'P_u' is the percentage of solvent uptake by the sample.

2.5. Kinetic studies

The mechanism of solvent uptake was studied by applying pseudo-first-order (PFO) and pseudo-second-order (PSO) kinetic models using the following expressions:[31]

Pseudo-first-order equation:

$$\ln (q_e - q_t) = \ln q_e - k_1 t$$

Pseudo-second-order equation:

$$\frac{t}{q_t} = \frac{1}{k_2 q_{e^2}} + \left(\frac{1}{q_e}\right) t$$

where 'q_e' and 'q_t' are the adsorption capacities in g g^{-1} at equilibrium and time t, respectively. k_1 (min^{-1}) is the rate constant for PFO adsorption and k_2 (g g^{-1} min^{-1}) is the rate constant for PSO adsorption.

2.6. Regeneration studies

The regeneration of the synthesized polymers for the adsorption of different organic solvents and petroleum products was examined by the squeezing method.[51,52] Excess oil was removed by squeezing the samples until a constant weight was attained. The samples were again dipped in various solvent–water emulsions separately under the optimized conditions of time and temperature. Swollen samples after immersion were again weighed and sorption capacities were calculated. This process was repeated until an appreciable adsorption capacity (more than 50%) was obtained.

2.7. Oil uptake in the oil–brine water system

Adsorption capacities of the optimized poly(EHA)-*cl*-C^h (2% MBA) and poly(MA)-*cl*-C^h (2% MBA) were recorded in diesel–brine water at different salt concentrations *i.e.*, 1%, 3%, and 5% at the optimized time and temperature to investigate the application of the synthesized polymers in marine oil spill clean-up.

3. Results and discussion

3.1. Synthesis and optimization

Various reaction conditions for the synthesis of oleophilic gels [poly(EHA)-*cl*-C^h and poly(MA)-*cl*-C^h] such as time, temperature, monomer concentration, and crosslinker concentration were optimized based on %grafting (Table 1). Initially, different reaction parameters were optimized to achieve maximum %grafting. The various reaction parameters include the temperature (70 °C to 90 °C) and reaction time (120 minutes to 30 minutes). Similarly, other parameters such as monomer [0.160–0.643 mol L^{-1}] and crosslinker concentrations [8.6–30.2 mmol L^{-1}] were also optimized subsequently to achieve maximum P_g. The optimized reaction conditions were found to be 120 min, 90 °C, 0.321 mol L^{-1} [EHA] and 8.6 mmol L^{-1} [MBA] for poly(EHA)-*cl*-C^h and 120 min, 70 °C, 0.73 mol L^{-1} [MA], and 8.6 mmol L^{-1} [MBA] for poly(MA)-*cl*-C^h. Poly(EHA)-*cl*-C^h and poly(MA)-*cl*-C^h synthesized with varied crosslinker concentrations [8.6 mmol L^{-1}, 21.6 mmol L^{-1}, 30.2 mmol L^{-1}, and 43.2 mmol L^{-1}] were further investigated for their oil adsorption capacity in different oils/organic solvents during adsorption studies.

3.2. Characterization

3.2.1. FTIR spectroscopy. The FTIR spectrum, as shown in Fig. 1, confirms the crosslinking of EHA and MA onto C^h. Here, the adsorption peak at 3321 cm^{-1} is due to hydrogen-bonded –OH groups. The peaks at 2928 cm^{-1} and 2925 cm^{-1} for poly(EHA)-*cl*-C^h and poly(MA)-*cl*-C^h, respectively, correspond to the –CH bond stretching of alkane. The change in the intensity of this peak in the IR spectrum of both poly(EHA)-*cl*-C^h and poly(MA)-*cl*-C^h confirms the incorporation of monomer moieties into the backbone.[53] The spectrum of the functionalized oleophilic gels exhibits a sharp peak at 1735 cm^{-1} corresponding to the –C═O stretching of the ester groups present in EHA and MA, implying the incorporation of ester groups into the backbone.[54] This was further supported by the presence of bands at 1154 cm^{-1} and 1156 cm^{-1}, corresponding to the –C–O–C stretching of esters in the case of poly(EHA)-*cl*-C^h and poly(MA)-*cl*-C^h, respectively.[53] The peak at 1232 cm^{-1} which corresponds to the lignin band (C–O stretching) in C^h is found missing in the case of poly(MA)-*cl*-C^h, confirming the changes associated with grafting reactions. The remaining peaks of other groups, which are common in both coconut husk and grafted samples, show only a little shift in their respective positions.

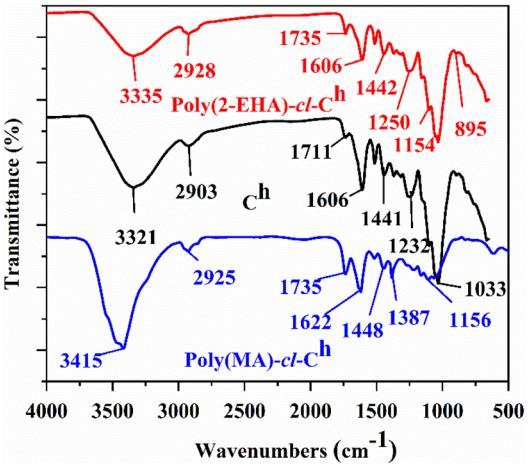

Fig. 1 FTIR spectra of C^h, poly(EHA)-*cl*-C^h and poly(MA)-*cl*-C^h.

3.2.2. FESEM. Changes in the surface morphology of the backbone and the oleophilic gels synthesized after the incor-

Table 1 Optimization of various reaction parameters for the synthesis of oleophilic gels, poly(EHA)-*cl*-C^h and poly(MA)-*cl*-C^h

	Poly(EHA)-*cl*-C^h					Poly(MA)-*cl*-C^h				
S. no.	Reaction temp. (°C)	Reaction time (min)	Monomer conc. (mol L^{-1})	Cross-linker conc. (mmol L^{-1})	P_g (%)	Reaction temp. (°C)	Reaction time (min)	Monomer conc. (mol L^{-1})	Cross-linker conc. (mmol L^{-1})	P_g (%)
1	70	120	0.321	8.6	20	70	120	0.73	8.6	94
2	80	120	0.321	8.6	30	80	120	0.73	8.6	75
3	90	120	0.321	8.6	90	90	120	0.73	8.6	70
4	90	90	0.321	8.6	10	70	90	0.73	8.6	50
5	90	60	0.321	8.6	25	70	60	0.73	8.6	42
6	90	30	0.321	8.6	28	70	30	0.73	8.6	33
7	90	120	0.160	8.6	20	70	120	0.367	8.6	44
8	90	120	0.643	8.6	50	70	120	1.47	8.6	28
9	90	120	0.321	21.6	80	70	120	0.73	21.6	67
10	90	120	0.321	30.2	70	70	120	0.73	30.2	76
11	90	120	0.321	43.2	65	70	120	0.73	43.2	60

Where no. of replications = 03, [KPS] = 2.46 mmol L^{-1}, and the weight of C^h = 1.00 g.

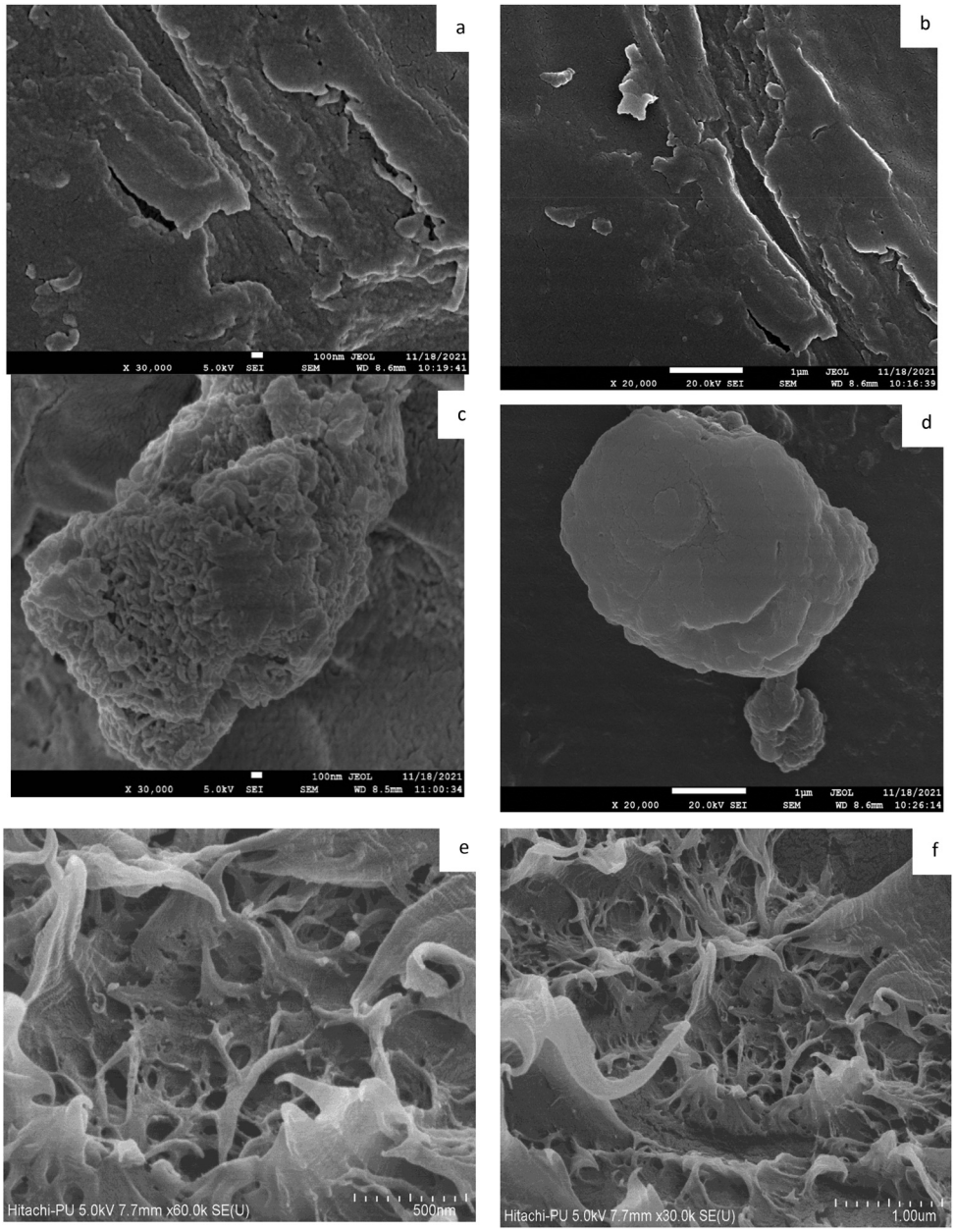

Fig. 2 SEM images of C^h (a and b), poly(EHA)-*cl*-C^h (c and d), and poly(MA)-*cl*-C^h (e and f).

poration of EHA and MA into C^h were analyzed by FESEM. Fig. 2a–d depict the FESEM images of C^h and poly(EHA)-*cl*-C^h, respectively, whereas Fig. 2e and f show the FESEM images of poly(MA)-*cl*-C^h. The micrograph of C^h showed a smooth and non-porous surface, while the surface of poly(EHA)-*cl*-C^h showed crosslinking networks having a porous surface. Similarly, FESEM images of poly(MA)-*cl*-C^h exhibited three-dimensional network formation due to crosslinking, and the crosslinks are much clearer at high magnification as shown in Fig. 2e. The porous three-dimensional network surface imparts high swelling characteristics in the crosslinked polymeric networks as compared to C^h because of the deep penetration and adsorption of oil into the polymeric networks through these pores.[55]

3.2.3. Energy dispersive X-ray spectroscopy (EDS) and mapping. Energy dispersive X-ray spectroscopy (EDS) and mapping were performed on pristine C^h and synthesized oleophilic gels to further confirm the crosslinking reactions and evaluate the presence of the desired elements incorporated into the backbone. The EDS spectra and mapping of C^h, poly(EHA)-*cl*-C^h, and poly(MA)-*cl*-C^h are shown in Fig. 3a–c, respectively. The EDS spectrum of both poly(EHA)-*cl*-C^h and poly(MA)-*cl*-C^h showed an additional peak of N (from MBA) along with peaks of C and O. Also, the wt% of C increased from 53.03 in

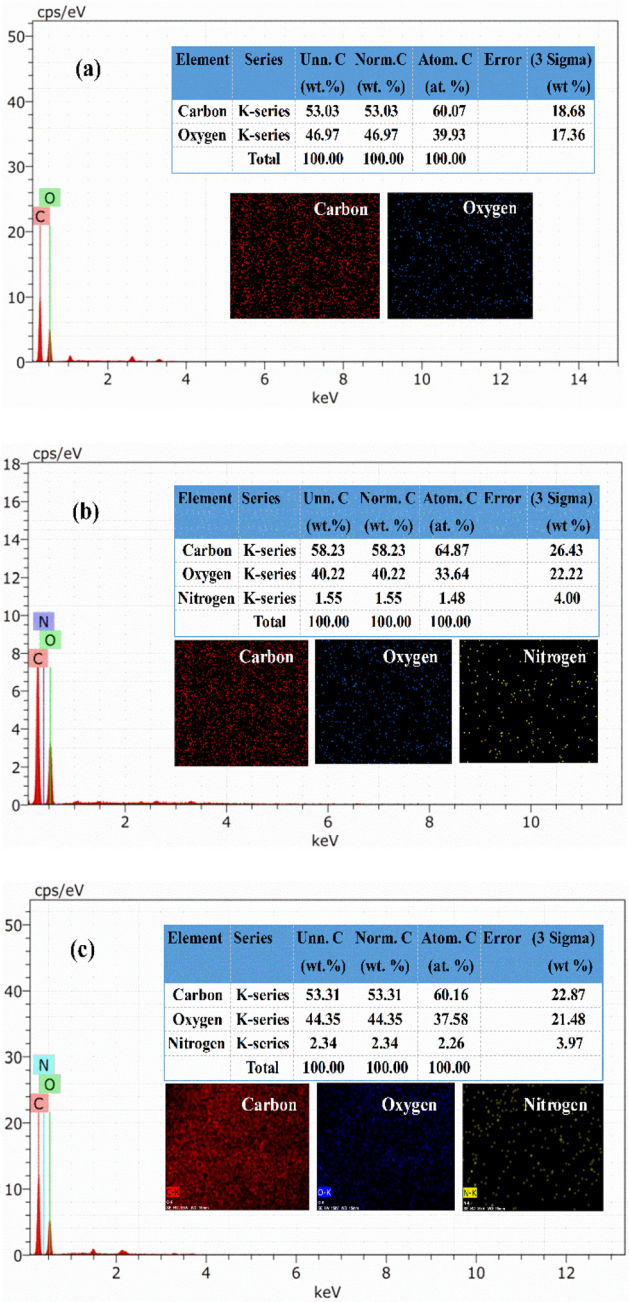

Fig. 3 EDS and mapping of C^h (a), poly(2-EHA)-*cl*-C^h (b), and poly(2-MA)-*cl*-C^h (c).

C^h to 58.23 and 53.31 in poly(EHA)-*cl*-C^h and poly(MA)-*cl*-C^h, respectively. Moreover, the higher wt% of carbon in poly(EHA)-*cl*-C^h as compared to that of poly(MA)-*cl*-C^h could be attributed to a longer hydrocarbon chain in EHA.

3.2.4. X-ray diffraction. The X-ray diffraction patterns of C^h, poly(EHA)-*cl*-C^h, and poly(MA)-*cl*-C^h are shown in Fig. 4. The XRD pattern of C^h shows sharp peaks indicating its crystalline nature, which is disturbed after the incorporation of the monomer moiety into it. Poly(EHA)-*cl*-C^h showed broad and less intense peaks at 2θ values of 19.28–23.7°, whereas poly

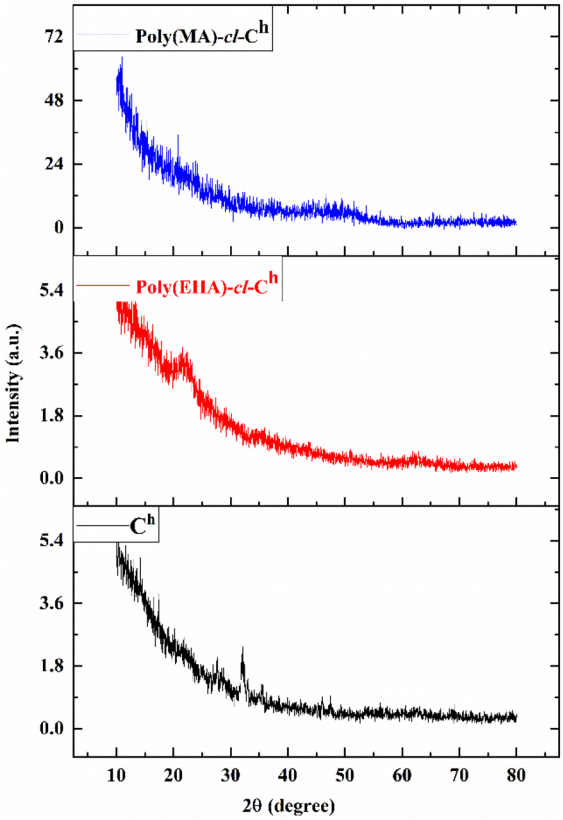

Fig. 4 XRD patterns of C^h, poly(EHA)-*cl*-C^h and poly(MA)-*cl*-C^h.

(MA)-*cl*-C^h showed these peaks at 2θ values of 40.02–50.1°. The broadness of the peaks confirmed the introduction of amorphous fractions into poly(EHA)-*cl*-C^h and poly(MA)-*cl*-C^h and supported the successful functionalization of C^h.[56]

3.3. Adsorption studies

The synthesized oleophilic gels were studied for the adsorption of different petroleum products (petrol, diesel, petroleum ether, and toluene). The synthesized matrices were subjected to batch adsorption studies in different oil–water emulsions to optimize the different adsorption conditions and to obtain the best absorbent out of all the synthesized polymers. Scheme 1 shows the comparison of the adsorption capacities of the synthesized oleophilic gels with that of pristine C^h in a diesel–water emulsion.

The adsorption capacity of pristine coconut husk is 2.1 g g^{-1} which is quite low in comparison with the adsorption capacities of poly(EHA)-*cl*-C^h (15.2 g g^{-1}) and poly(*MA*)-*cl*-C^h (13.0 g g^{-1}). The introduction of the hydrophobic character with the increase in the hydrocarbon part of the monomer resulted in an increased oleophilic character of the matrix. The synthesized polymers are, therefore, efficient and far better as an oil adsorbent as compared to the backbone used.

The optimization studies of the adsorption conditions such as contact time and temperature for poly(EHA)-*cl*-C^h and poly (*MA*)-*cl*-C^h are discussed as follows.

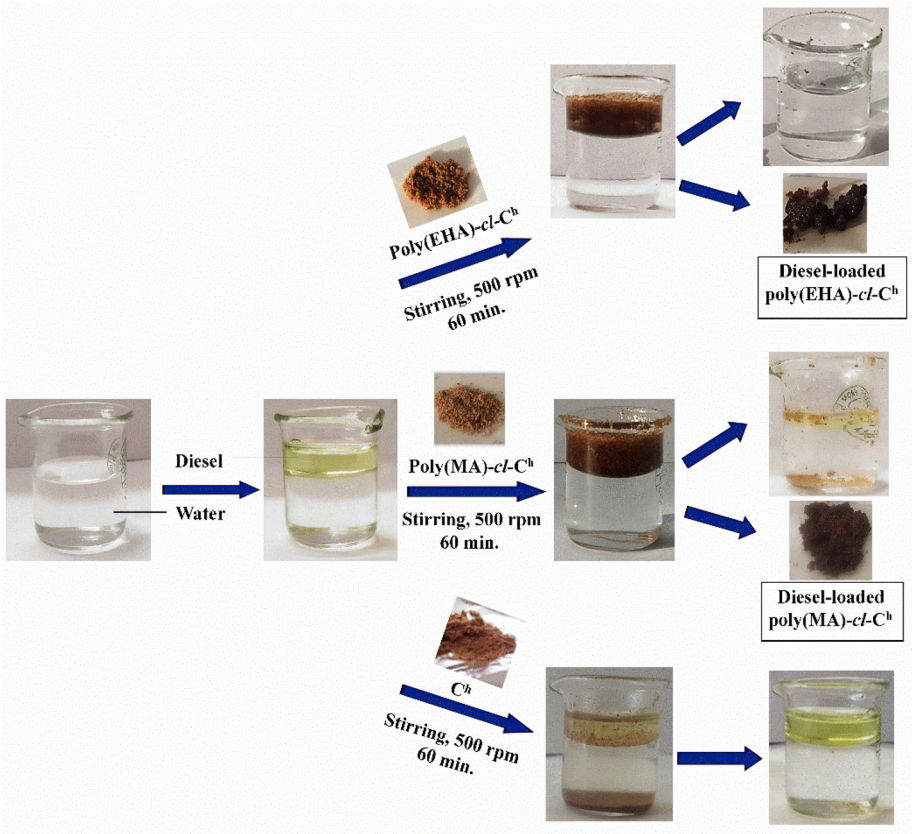

Scheme 1 Adsorption of oil from oil–water emulsions with poly(EHA)-*cl*-C^h, poly(MA)-*cl*-C^h, and pristine C^h, the backbone.

3.3.1. Effect of contact time. The effect of contact time (30 min–210 min) on the adsorption of petrol, diesel, petroleum ether, and toluene was studied using different oleophilic gels synthesized at varied crosslinker (MBA) concentrations *i.e.*, 2%, 5%, 7%, and 10%, to evaluate the effect of crosslinking density on the adsorption besides contact time at 25 °C (Fig. 5 and 6). The polymers with crosslinker concentrations having the best adsorption capacities were selected for further optimization studies. The sorption capacity of the oleophilic gels increased with an increase in time until equilibrium and then decreased. The optimized time for all poly(EHA)-*cl*-C^h polymers with different MBA concentrations was found to be 60 min for diesel and 90 min for petrol, toluene, and petroleum ether uptake. However, the optimized time for all poly(MA)-*cl*-C^h polymers with different MBA concentrations was found to be 60 min for all the solvents. It was observed that poly(EHA)-*cl*-C^h (2% MBA) showed maximum sorption capacities of 15.00 g g^{-1} (diesel–water), 13 g g^{-1} (petrol–water), 10.4 g g^{-1} (toluene–water), and 9.4 g g^{-1} (petroleum ether–water), whereas poly(MA)-*cl*-C^h (2% MBA) showed maximum adsorption capacities of 12.2 g g^{-1} (diesel–water), 10.8 g g^{-1} (petrol–water), 8.8 g g^{-1} (toluene–water), and 8.2 g g^{-1} (petroleum ether–water). The observed trend of oil uptake is due to the availability of a large number of vacant sites on sorbents at the beginning, which got occupied with time until equilibrium was reached where all the adsorption sites got saturated with oil.[1] It was also observed that with the increase in crosslinker concentration, there is a reduction in the adsorption capacity because with the increase in the crosslinker concentration, the network structure becomes more compact leading to condensed pore size and less adsorption capacity.[57] The higher sorption capacities of EHA-crosslinked polymers as compared to those of MA-crosslinked polymers could be due to the presence of a bulky alkyl chain (2-ethylhexyl group) in EHA, introducing more hydrophobicity as compared to the small alkyl part (methyl group) in MA.[58]

The optimized time and crosslinker concentrations were selected for further optimization of temperature and kinetic studies.

3.3.2. Effect of temperature. The effect of the temperature variation was studied in the range of 25–45 °C at the optimized time and crosslinker concentration. It was found that the adsorption capacity of poly(EHA)-*cl*-C^h initially increased with an increase in temperature from 15.0 g g^{-1} (25 °C) to 15.2 g g^{-1} (30 °C) for diesel–water, 13.0 g g^{-1} (25 °C) to 13.4 g g^{-1} (30 °C) for petrol–water, 10.4 g g^{-1} (25 °C) to 11.0 g g^{-1} (30 °C) for toluene–water, and 9.4 g g^{-1} (25 °C) to 10.4 g g^{-1} (35 °C) for petroleum ether–water, and then decreased gradually on a further rise in temperature (Fig. 7a). Similarly, the adsorption capacity of poly(MA)-*cl*-C^h showed an increase with the

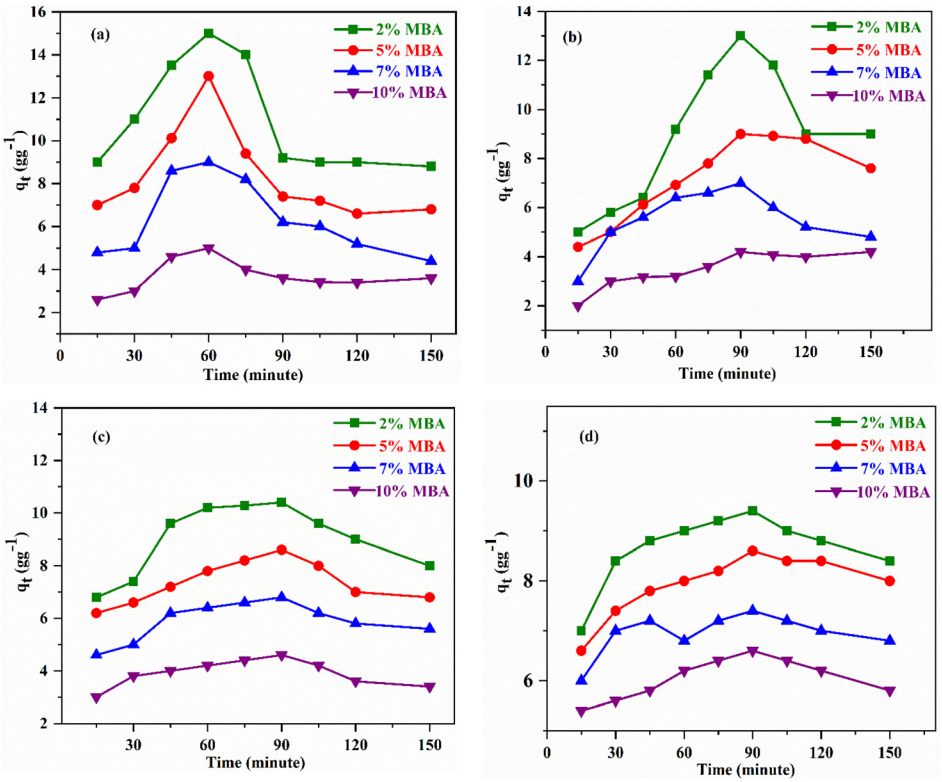

Fig. 5 Adsorption of (a) diesel, (b) petrol, (c) toluene, and (d) petroleum ether by poly(EHA)-*cl*-C^h with respect to time at 25 °C.

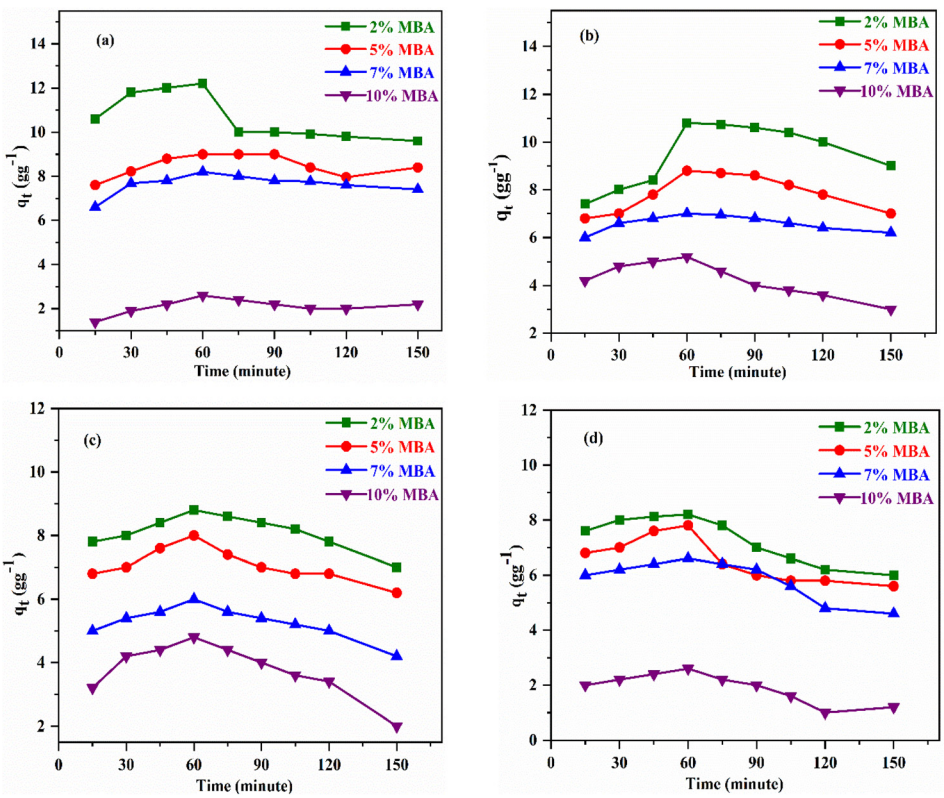

Fig. 6 Adsorption of (a) diesel, (b) petrol, (c) toluene, and (d) petroleum ether by poly(MA)-*cl*-C^h with respect to time at 25 °C.

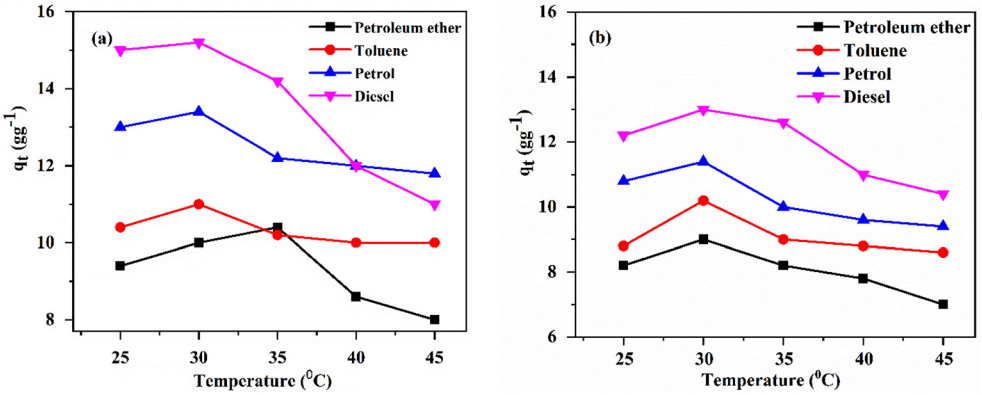

Fig. 7 Adsorption with respect to temperature by (a) poly(EHA)-*cl*-C^h (2% MBA) and (b) poly(MA)-*cl*-C^h (2% MBA) at 60 min.

increase in the temperature from 12.2 g g^{-1} (25 °C) to 13.0 g g^{-1} (30 °C) for diesel–water, 10.8 g g^{-1} (25 °C) to 11.4 g g^{-1} (30 °C) for petrol–water, 8.8 g g^{-1} (25 °C) to 10.2 g g^{-1} (30 °C) for toluene–water, and 8.2 g g^{-1} (25 °C) to 9.0 g g^{-1} (35 °C) for petroleum ether–water, and then decreased gradually on a further rise in temperature (Fig. 7b).

A temperature rise resulted in a decreased viscosity of the oil which increased its diffusion into the polymeric matrix. On a further rise in temperature, the rate of desorption increases considerably due to an increase in the kinetic energy of the sorbate present on the surface of the sorbent. Thus, above the optimized temperature, retention of oil or organic fluids by polymeric samples becomes difficult.[1]

Various lignocellulosic biowastes have been found to exhibit sorption of oils from oily wastewater solutions and their sorption capacities, in particular oils, are compared with the oleophilic gels synthesized in the present study as shown in Table 2.

3.3.3. Kinetic studies. The pseudo-first-order (PFO) and pseudo-second-order (PSO) kinetic models were applied to time studies to understand the nature of interactions between the sorbate and the sorbent (Fig. 8). Correlation coefficients (R^2) calculated from PFO and PSO for poly(EHA)-*cl*-C^h (2% MBA) were found to be 0.8638 and 0.9718 in diesel, 0.88442 and 0.90123 in petrol, 0.22809 and 0.97674 in toluene, and 0.56031 and 0.99699 in petroleum ether, respectively (Table 3). Similarly, R^2 calculated from PFO and PSO for poly(MA)-*cl*-C^h (2%MBA) were found to be 0.12939 and 0.98237 in diesel, 0.51289 and 0.97737 in petrol, 0.09797 and 0.99609 in toluene, and 0.21853 and 0.97757 in petroleum ether, respectively. The R^2 value is closer to 1.0 for PSO in all the cases, hence, the adsorption process is best fitted in the PSO kinetics model, which implies that there must be some chemical interactions between the sorbate and the sorbent causing the adsorption of oil by polymers.[63]

3.3.4. Regeneration studies. Since the oleophilic gels showed maximum adsorption capacity in the case of diesel–oil, the reusability of poly(EHA)-*cl*-C^h and poly(MA)-*cl*-C^h as diesel–oil sorbents was studied by the simple squeezing method. Poly(EHA)-*cl*-C^h showed an adsorption capacity of 5.0 g g^{-1} even after the 6th cycle of adsorption and the sorption capacity of poly(MA)-*cl*-C^h was found to be 3.2 g g^{-1} after the 5th cycle of repeatability as shown in Fig. 9. The cumulative adsorption capacities of poly(EHA)-*cl*-C^h and poly(MA)-*cl*-C^h were found to be 50.0 g g^{-1} and 35.2 g g^{-1}, respectively. Thus, the synthesized polymers were found to be reusable and efficient adsorbers of oil from oily wastewater.

3.3.5. Oil uptake in brine solution. The adsorption behaviour of poly(EHA)-*cl*-C^h (2% MBA) and poly(MA)-*cl*-C^h (2% MBA) in a brine water–diesel emulsion was investigated at different salt concentrations (1, 3, and 5%) and is shown in Table 4. The study was performed with a diesel–brine water emulsion as both the oleophilic gels showed maximum adsorption capacities in the diesel–water emulsion. From the

Table 2 Comparison of oil sorption capacities of different sorbents

S. no.	Sorbent	Oil	Equilibrium adsorption capacity (q_e in g g^{-1})	Ref.
1	Modified orange peel	Weathered crude oil	4.78	7
2	Modified rice husk	Heavy crude oil	6.00	58
3	Modified sugarcane bagasse	Vegetable oil	5.6–6.3	59
4	*Solanum incanum* leaves	Motor oil	11.54	1
5	Treated mango peel	Crude oil	0.3	59
6	Corn waste biochar	Oil	6.00–8.00	60
7	Esterified durian peels	Diesel oil	0.3780	61
8	Walnut shell	Vegetable oil	0.51	62
9	**Coconut husk (EHA crosslinked) 2% MBA**	**Diesel oil**	**15.2**	**Present work**
10	**Coconut husk (MA crosslinked) 2% MBA**	**Diesel oil**	**13.0**	**Present work**

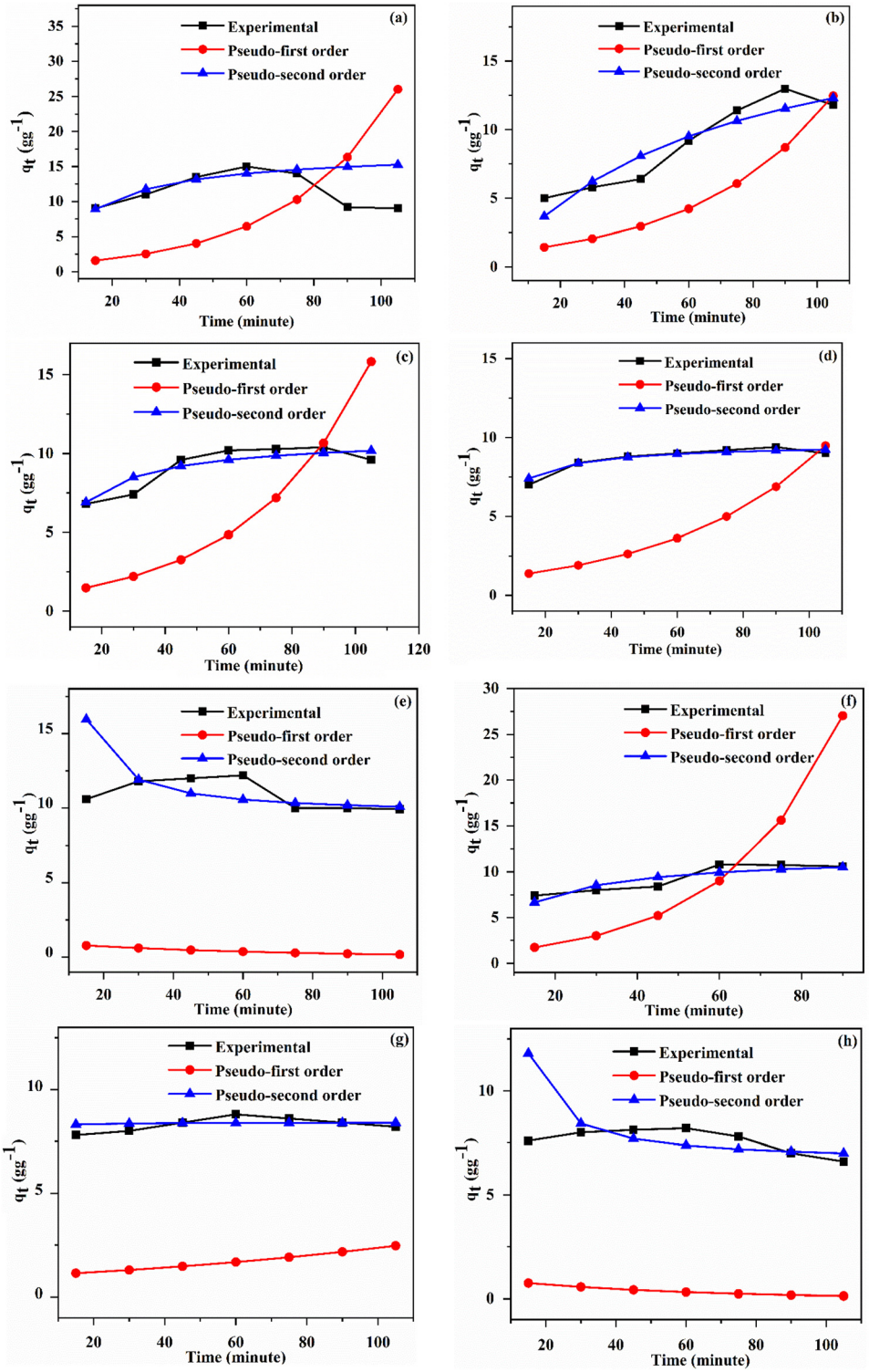

Fig. 8 Compiled kinetic models of poly(EHA)-*cl*-C^h (2% MBA) for sorption of (a) diesel, (b) petrol, (c) toluene, and (d) petroleum ether, and poly (MA)-*cl*-C^h (2% MBA) for sorption of (e) diesel, (f) petrol, (g) toluene, and (h) petroleum ether.

data obtained, it can be concluded that poly(EHA)-*cl*-C^h (2% MBA) and poly(MA)-*cl*-C^h (2% MBA) show considerable oil uptake in the oil–salt emulsion, which is comparable to that observed in the emulsion of oil and distilled water. Hence, the synthesized polymers can also act as suitable candidates for oil spill cleanup from marine water bodies.

Table 3 Parameters of the adsorption kinetics for adsorption of different organic solvents

Organic solvent	Kinetic models applied	Kinetics parameters	Poly(EHA)-*cl*-C^h (2% MBA)	Poly(MA)-*cl*-C^h (2% MBA)
Diesel	Pseudo-first order	q_e (g g^{-1})	0.777608	0.39698
		K_1 (min^{-1})	0.03104	−0.01636
		R^2	0.8638	0.12939
	Pseudo-second order	q_e (g g^{-1})	17.33403	9.50751
		K_2 (g g^{-1} min^{-1})	0.004055	−0.01735
		R^2	0.9718	0.98237
Petrol	Pseudo-first order	q_e (g g^{-1})	14.06248	6.23257
		K_1 (min^{-1})	0.02404	0.03664
		R^2	0.88442	0.51289
	Pseudo-second order	q_e (g g^{-1})	20.24701	11.89343
		K_2 (g g^{-1} min^{-1})	0.00073	0.007125
		R^2	0.90123	0.97737
Toluene	Pseudo-first order	q_e (g g^{-1})	0.137281	0.83526
		K_1 (min^{-1})	0.0263	0.0086
		R^2	0.22809	0.09797
	Pseudo-second order	q_e (g g^{-1})	11.05217	8.41042
		K_2 (g g^{-1} min^{-1})	0.010029	0.65662
		R^2	0.97674	0.99609
Petroleum ether	Pseudo-first order	q_e (g g^{-1})	−0.40702	0.13799
		K_1 (min^{-1})	0.02143	−0.01937
		R^2	0.56031	0.21853
	Pseudo-second order	q_e (g g^{-1})	9.629273	6.55308
		K_2 (g g^{-1} min^{-1})	0.023074	−0.02286
		R^2	0.99699	0.97757

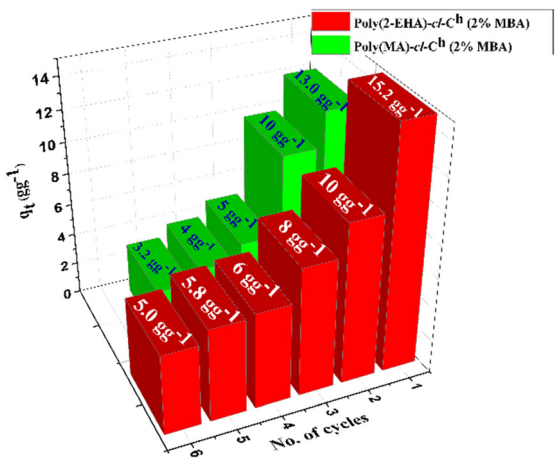

Fig. 9 Reusability studies of poly(EHA)-*cl*-C^h (2% MBA) and poly(MA)-*cl*-C^h (2% MBA) in diesel oil.

Table 4 Adsorption capacities of poly(EHA)-*cl*-C^h (2% MBA) and poly (MA)-*cl*-C^h (2% MBA) in the diesel–brine water system

Poly(EHA)-*cl*-C^h (2% MBA)		Poly(MA)-*cl*-C^h (2% MBA)	
Brine solution concentration	q_t (g g^{-1})	Brine solution concentration	q_t (g g^{-1})
1%	15	1%	12.2
3%	14.1	3%	11
5%	12.8	5%	10.4

4. Conclusions

Pristine coconut husk and hydrophobic acrylate (EHA and MA)-based oleophilic gels were synthesized using a free radical polymerization technique with KPS–MBA as an initiator–cross-linker system. During synthesis, different reaction conditions were optimized to obtain the best %grafting values. The optimized reaction conditions were 120 min, 90 °C, 0.321 mol L^{-1} [EHA] and 8.6 mmol L^{-1} [MBA] for poly(EHA)-*cl*-C^h and 120 min, 70 °C, 0.73 mol L^{-1} [MA], and 8.6 mmol L^{-1} [MBA] for poly(MA)-*cl*-C^h, respectively. The synthesized gels were characterized using FTIR, FESEM, EDS-mapping, and XRD analysis and were examined for the uptake of various organic solvents and oils (petrol, diesel, petroleum ether, and toluene) from wastewater. It was observed that, unlike coconut husk, these polymeric networks were hydrophobic. Owing to their greater hydrophobic nature, the poly(EHA)-*cl*-C^h networks exhibited higher oil uptake capacity than poly(MA)-*cl*-C^h. Also in each case, the polymer with the MBA concentration (2%) showed a maximum sorption capacity of 15.2 g g^{-1} for poly (EHA)-*cl*-C^h and 13.0 g g^{-1} for poly(MA)-*cl*-C^h in diesel oil within 60 minutes, in comparison with the pristine coconut husk, the backbone, exhibiting only 2.1 g g^{-1} maximum adsorption capacity. Both the oleophilic gels followed PSO kinetics for adsorption and appreciable adsorption properties up to six cycles of reusability with cumulative adsorption capacities of 50.0 g g^{-1} and 35.2 g g^{-1} for poly(EHA)-*cl*-C^h and poly(MA)-*cl*-C^h, respectively. The oleophilic gels showed comparable adsorption capacities of 15.0 g g^{-1} and 12.2 g g^{-1} for poly(EHA)-*cl*-C^h and poly(MA)-*cl*-C^h, respectively, even in brine water–oil emulsions. Since the synthesized oleophilic gels show high adsorption towards different candidate petroleum products, they can be used as suitable candidates for oil spill remediation. The gels also show remarkable oil adsorption in the brine water emulsion, which enhances their applicability in marine oil spill incidents. The recyclability of the gels with appreciable adsorption up to six repeated cycles is quite

remarkable. The green synthetic methods involved in the synthesis of the oleophilic gels make them environmentally friendly. Thus, the synthesized oleophilic gels are efficient oil adsorbents and will have a significant societal impact.

Author contributions

Kavita Devi: experimental work and draft manuscript writing; Ghanshyam S. Chauhan: conceptualization, manuscript revision, and editing; Sunita Ranote: investigation, methodology, and data calculation; Sandeep Chauhan: co-supervision, conceptualization, and writing – editing; Kiran Kumar: supervision, conceptualisation, and writing – editing.

Conflicts of interest

The authors have no conflicts of interest to declare that are relevant to the contents of this article.

References

1 A. Abutaleb, N. Zouli, O. Y. Bakather and M. A. Mahmoud, *Desalin. Water Treat.*, 2021, **233**, 182, DOI: **10.5004/dwt.2021.27529**.
2 S. Fürtauer, M. Hassan, A. Elsherbiny, S. A. Gabal, S. Mehanny and H. Abushammala, *Polymers*, 2021, **13**, 2739, DOI: **10.3390/polym13162739**.
3 A. Jernelv, *Ambio*, 2010, **39**, 353, DOI: **10.1007/s13280-010-0085-5**.
4 I. Aa, A. Op, I. Ujj and B. Mt, *Environ. Monit. Assess.*, 2022, **194**, 816, DOI: **10.1007/s10661-022-10424-x**.
5 S. M. Techtmann, J. S. Domingo, R. Conmy and M. Barron, *Appl. Microbiol. Biotechnol.*, 2023, **107**, 1095–1106, DOI: **10.1007/s00253-022-12332-z**.
6 V. Sharma, A. Ramish and O. Sahu, *J. Oil Gas Petrochem. Sci.*, 2021, **3**, 1, DOI: **10.30881/jogps.00029**.
7 I. A. El Gheriany, F. Ahmad El Saqa, A. Abd El Razek Amer and M. Hussein, *Alexandria Eng. J.*, 2020, **59**, 925, DOI: **10.1016/j.aej.2020.03.024**.
8 M. Zamparas, D. Tzivras, V. Dracopoulos and T. Ioannides, *Molecules*, 2020, **25**, 1, DOI: **10.3390/molecules25194522**.
9 I. C. Ossai, A. Ahmed, A. Hassan and F. S. Hamid, *Environ. Technol. Innovation*, 2020, **17**, 100526, DOI: **10.1016/j.eti.2019.100526**.
10 M. Fouladi, M. K. Heidari and O. Tavakoli, *J. Porous Mater.*, 2023, **30**(3), 1037, DOI: **10.1007/s10934-022-01385-0**.
11 S. F. A. Ali and W. K. Hassan, *J. Eng. Res.*, 2019, **7**, 85, DOI: **10.30918/AJER.73.19.032**.
12 Saruchi, V. Kumar, A. A. Ghfar and S. Pandey, *Biomass Convers. Biorefin.*, 2023, **13**, 383–392, DOI: **10.1007/s13399-022-02665-0**.
13 B. He, Y. Zhang, B. Li, Y. Chen and L. Zhu, *J. Environ. Chem. Eng.*, 2021, **9**, 106333, DOI: **10.1016/j.jece.2021.106333**.
14 K. Jayaramulu, F. Geyer, M. Petr, R. Zboril, D. Vollmer and R. A. Fischer, *Adv. Mater.*, 2017, **29**, 1605307, DOI: **10.1002/adma.201605307**.
15 A. M. Tayeb, R. Farouq, O. A. Mohamed and M. A. Tony, *Int. J. Environ. Anal. Chem.*, 2020, **100**, 311, DOI: **10.1080/03067319.2019.1636976**.
16 R. Asadpour, N. Sapari, M. H. Isa, S. Kakooei, K. U. Orji and S. Daneshfozoun, *Adv. Mater. Res.*, 2016, **1133**, 552, DOI: **10.4028/www.scientific.net/amr.1133.552**.
17 J. C. Onwuka, E. B. Agbaji, V. O. Ajibola and F. G. Okibe, *BMC Chem.*, 2019, **13**, 1, DOI: **10.1186/s13065-019-0593-8**.
18 G. Alaa El-Din, A. A. Amer, G. Malsh and M. Hussein, *Alexandria Eng. J.*, 2018, **57**, 2061, DOI: **10.1016/j.aej.2017.05.020**.
19 P. de la Concepción Martínez-Nodal, I. L. Rodríguez-Rico, E. R. Domínguez and L. Rodríguez-Machín, *Water, Air, Soil Pollut.*, 2022, **233**, 149, DOI: **10.1007/s11270-022-05584-y**.
20 A. B. Daniel, E. Zahir and M. A. Asghar, *Pet. Sci. Technol.*, 2019, **37**, 1143, DOI: **10.1080/10916466.2019.1578797**.
21 R. Kandanelli and C. S. K. Raju, *Environ. Sci.: Adv.*, 2023, **2**, 339, DOI: **10.1039/d2va00167e**.
22 K. G. Akpomie and J. Conradie, *Populus nigra* leaf-derived biochar: an efficient and reusable low-cost carbon material for the ultrasonic-assisted remediation of oil spill, *Biomass Convers. Biorefin.*, 2022, 1–13, DOI: **10.1007/s13399-022-02350-2**.
23 U. Michael-igolima, S. J. Abbey, A. O. Ifelebuegu and E. U. Eyo, *Materials*, 2023, **16**(3), 1092, DOI: **10.3390/ma16031092**.
24 X. Yue, T. Zhang, D. Yang, F. Qiu and Z. Li, *J. Cleaner Prod.*, 2018, **199**, 411, DOI: **10.1016/j.jclepro.2018.07.181**.
25 Z. Wang, J. Saleem, J. P. Barford and G. McKay, *Environ. Technol.*, 2020, **41**, 1980, DOI: **10.1080/09593330.2018.1552725**.
26 B. M. Omar, S. A. Abdelgalil, H. Fakhry, T. M. Tamer and M. A. El-Sonbati, *Sci. Rep.*, 2023, **13**, 1, DOI: **10.1038/s41598-023-29035-8**.
27 F. Liu, R. Jamal, T. Abdiryim and X. Liu, *Cellulose*, 2022, Springer Netherlands. DOI: **10.1007/s10570-022-04787-0**.
28 A. A. A. Aziz and M. F. Mohamad, *Proc. Sci. Math.*, 2022, **14**, 47–55.
29 B. Y. Eweida, A. M. Omer, T. M. Tamer, H. A. E. M. Soliman, A. A. Zaatot and M. S. Mohy-Eldin, *Polym. Bull.*, 2023, **80**, 4813–4840, DOI: **10.1007/s00289-022-04260-9**.
30 N. T. Tung, N. T. Duc, P. T. T. Ha, L. D. Giang, H. T. Van An and N. T. Son, *Cellul. Chem. Technol.*, 2022, **56**, 461, DOI: **10.35812/cellulosechemtechnol.2022.56.39**.
31 M. R. Krishnan, Y. F. Aldawsari and E. H. Alsharaeh, *J. Appl. Polym. Sci.*, 2021, **138**, 1, DOI: **10.1002/app.49942**.
32 S. Ranote, S. Chauhan, K. Kumar and G. S. Chauhan, *Bioresour. Technol. Rep.*, 2023, **22**, 101417, DOI: **10.1016/j.biteb.2023.101417**.
33 S. Kumari, G. S. Chauhan, S. Monga, A. Kaushik and J. H. Ahn, *RSC Adv.*, 2016, **6**, 77768, DOI: **10.1039/C6RA13308H**.

34 B. Ram, S. Jamwal, S. Ranote, G. S. Chauhan and R. Dharela, *ACS Appl. Polym. Mater.*, 2020, **2**, 5290, DOI: **10.1021/acsapm.0c01025**.
35 K. Muthumani and V. Sathuragiri, *World Wide J. Multidiscip. Res. Dev.*, 2022, **8**, 61.
36 N. E. Ekpenyong, *Brill. Eng.*, 2021, **3**, 1, DOI: **10.36937/ben.2022.4547**.
37 O. S. Bello, K. A. Adegoke, S. O. Fagbenro and O. S. Lameed, *Appl. Water Sci.*, 2019, **9**, 1, DOI: **10.1007/s13201-019-1051-4**.
38 A. O. Ifelebuegu and Z. Momoh, Proc. of the Intl. Conf. on Advances in Applied Science and Environmental Technology - ASET 2015, 2015, 10–15.DOI: **10.15224/978-1-63248-040-8-38**.
39 X. Zhang, X. Kang, J. Mi, J. Jin and H. Meng, *Sep. Purif. Technol.*, 2023, **324**, 124623, DOI: **10.1016/j.seppur.2023.124623**.
40 Y. Jiang, Y. Jiang, C. Su, X. Sun, Y. Xu, S. Cheng, Y. Liu, X. Dou and Z. Yang, *Fuel*, 2024, **355**, 129402, DOI: **10.1016/j.fuel.2023.129402**.
41 J. Tang, L. Zhao, S. Jiang, Y. Huang, J. Zhang and J. Li, *Appl. Surf. Sci.*, 2023, **639**, 158194, DOI: **10.1016/j.apsusc.2023.158194**.
42 E. David and V.-C. Niculescu, *Int. J. Environ. Res. Public Health*, 2021, **18**(24), 13147, DOI: **10.3390/ijerph182413147**.
43 Y.-J. Tu, C.-K. Chang and C.-F. You, *J. Hazard. Mater.*, 2012, **229–230**, 258–264, DOI: **10.1016/j.jhazmat.2012.05.100**.
44 S. Jiang, L. Zhang, L. Zhao, J. Zhang and Y. Huang, *Chem. Eng. J.*, 2023, **474**, 145979, DOI: **10.1016/j.cej.2023.145979**.
45 C. Corsaro, G. Neri, A. Santoro and E. Fazio, *Materials*, 2022, **15**, 282, DOI: **10.3390/ma15010282**.
46 X. P. Nguyen, D. T. Nguyen, V. V. Pham and D. T. Vo, *Water Conserv. Manag.*, 2022, **6**, 6, DOI: **10.26480/wcm.01.2022.06.14**.
47 W. Al-Mughrabi, A. O. Al-Dossary and A. Abdel-Naby, *Polymers*, 2022, **14**, 1, DOI: **10.3390/polym14091707**.
48 M. Gandara, D. R. Mulinari, F. M. Monticeli and M. R. Capri, *J. Nat. Fibers*, 2021, **18**, 1983, DOI: **10.1080/15440478.2019.171065**.
49 G. Akhlamadi and E. K. Goharshadi, *Process Saf. Environ. Prot.*, 2021, **154**, 155, DOI: **10.1016/j.psep.2021.08.009**.
50 D. T. Tran, S. T. Nguyen, N. D. Do, N. N. T. Thai, Q. B. Thai, H. K. P. Huynh, V. T. T. Nguyen and A. N. Phan, *Mater. Chem. Phys.*, 2020, **253**, 123363, DOI: **10.1016/j.matchemphys.2020.123363**.
51 M. O. Adebajo, R. L. Frost, J. T. Kloprogge, O. Carmody and S. Kokot, *J. Porous Mater.*, 2003, **10**, 159.
52 D. Wu, L. Fang, Y. Qin, W. Wu, C. Mao and H. Zhu, *Mar. Pollut. Bull.*, 2014, **84**, 263–267, DOI: **10.1016/j.marpolbul.2014.05.005**.
53 K. Patidar and M. Vashishtha, *J. Serb. Chem. Soc.*, 2021, **86**, 429.
54 N. Munir, K. B. Lodge, B. Hinderliter, M. A. Maurer-Jones and R. Duckworth, International conference (19th) on environmental degradation of materials in nuclear power systems - Water Reactors (EnvDeg), Boston, United States, 2019, 899–905.
55 A. G. Ibrahim, A. Z. Sayed, H. A. El-wahab and M. M. Sayah, *Int. J. Biol. Macromol.*, 2020, **159**, 422, DOI: **10.1016/j.ijbiomac.2020.05.039**.
56 J. S. A. Cortez, B. I. Kharisov, T. Serrano, L. T. González, O. V. Kharissova, J. S. Acevedo, B. I. Kharisov, T. Serrano, T. Lucy and O. V. Kharissova, *J. Dispersion Sci. Technol.*, 2019, **40**, 884, DOI: **10.1080/01932691.2018.148859**.
57 Y. Yang, A. K. N. Nair and S. Sun, *Ind. Eng. Chem. Res.*, 2019, **58**, 8426, DOI: **10.1021/acs.iecr.9b00690**.
58 S. Kumagai, Y. Noguchi, Y. Kurimoto and K. Takeda, *Waste Manage.*, 2007, **27**, 554.
59 U. Ismail, W. N. Kamaruzaman and Z. C. Will, *Int. Res. J. Eng. Technol.*, 2020, **07**, 1311.
60 A. Khokhlov and L. Khokhlova, *Technol. Audit Prod. reserves*, 2021, **4**, 21, DOI: **10.15587/2706-5448.2021.238342**.
61 V. N. Thai, T. N. Trinh, N. D. Dao and T. H. P. Pham, *Chem. Eng. Trans.*, 2020, **78**, 271, DOI: **10.3303/CET2078046**.
62 A. Srinivasan and T. Viraraghavan, *Bioresour. Technol.*, 2008, **99**, 8217, DOI: **10.1016/j.biortech.2008.03.072**.
63 X. Sun, H. Fu, M. Bao, W. Liu, C. Luo, Y. Li, Y. Li and J. Lu, *BioChar*, 2022, **4**, 60, DOI: **10.1007/s42773-022-00184-9**.